Available online at www.sciencedirect.com
ScienceDirect
Trans. Nonferrous Met. Soc. China 22(2012) 496−502
Transactions of Nonferrous Metals Society of China
www.tnmsc.cn

Microstructure and texture of commercially pure titanium in cold deep drawing

ZHANG Xu-hu, TANG Bin, ZHANG Xia-lu, KOU Hong-chao, LI Jin-shan, ZHOU Lian

State Key Laboratory of Solidification Processing, Northwestern Polytechnical University, Xi'an 710072, China

Received 21 January 2011; accepted 10 December 2011

Abstract: The development of microstructure and texture during cold deep drawing of commercially pure titanium (CP-Ti) was investigated. Three parts, stretching region, drawing region and flange region, were sequentially formed in the deep drawing process of the hemispheric surface part, with reference to deformation modes and strain regimes. Results show that the plastic strain is accommodated by dislocation slip and deformation twinning in the whole deep drawing process. The texture of the CP-Ti sheet and its drawn part consists of rolling texture component and recrystallization texture component. The intensity and type of the initial texture varied during the drawing process are related to the production of deformation twinning and dislocation slip. Twinning weakens the initial texture by randomizing the orientations of crystals, especially for the recrystallization texture. The recrystallization texture in the drawing region disappears due to the significant forming of twinning. Furthermore, over drawing would result in the predominance of dislocation slip and the texture is strengthened.

Key words: pure titanium; deep drawing; microstructure; texture

1 Introduction

Recently, commercial pure titanium (CP-Ti) drawn part has been widely applied in the chemical [1,2] and aerospace [3,4] industries due to its corrosion resistance, good welding property, low density and high specific strength. Because of its hexagonal close-packed (HCP) crystal structure, CP-Ti has more complex deformation mechanisms than those cubic metals, therefore exhibits limited ductility and anisotropic mechanical properties at room temperature. In order to improve the formability of CP-Ti, lots of research focused on the deformation and transformation mechanisms in rolling, heating and cooling process [5−8]. Besides, in order to achieve a homogeneous microstructure composed of ultrafine grains, the evolution of microstructure and texture of the CP-Ti was widely investigated, especially for severe plastic deformation, such as high-ratio differential speed rolling [9], superplastic forming [10] and equal channel angular extrusion [11].

Although the warm and hot forming can improve the formability, the cold drawing is always desired for the cost-effective reason, whereas the forming of CP-Ti cups [2,12] and thin-walled hemispheric surface part are the typical applications [13]. The forming process of the hemispheric surface part is different from the normal deep drawing such as square or cylindrical drawn part. It is a complex process comprised by stretching and drawing [14]. However, there are few literatures focusing on the microstructure and texture development of the CP-Ti in the forming process of the hemispheric surface part.

In order to avoid the deep drawing defect and obtain the homogeneous microstructure, the deformation process of the hemispheric surface part was investigated by finite element method (FEM) and the parameters were optimized by orthogonal tests in our previous work [15].

In the present work, the evolution of microstructure and texture in the drawing process of hemispheric surface part was investigated using experimental approach. The microstructure at different regions of the drawn part was obtained by optical microscopy (OM) and transmission electron microscopy (TEM). Textures were measured using X-ray diffraction. Based on the experimental results, the effect of deformation twinning and dislocation slip on texture development was analyzed.

Foundation item: Project (SKLSP200906) supported by the Fund of State Key Laboratory of Solidification Processing in NWPU; Project (B08040) supported by Program of Introducing Talents of Discipline in the Project of Advanced Materials and Their Forming Technology
Corresponding author: TANG Bin; Tel: +86-29-88460361; Fax: +86-29-88460294; E-mail: toby198489@163.com
DOI: 10.1016/S1003-6326(11)61204-1

2 Experimental

2.1 Initial materials

The pure titanium sheets used in this investigation were obtained in the form of 0.95 mm in thickness, which were formed by multi-direction cold rolling and subsequently annealing. The chemical composition is shown in Table 1.

Table 1 Chemical composition of CP-Ti sheets (mass fraction, %)

C	Fe	H	N	O	Ti
0.01	0.043	0.004	0.01	0.17	Bal.

Figure 1(a) shows the initial microstructure of CP-Ti sheet. It can be seen that the initial CP-Ti sheet has equiaxed grain with size of 20 μm. The texture of the sheet is detected by XRD technique and the (0002) pole figure is shown in Fig. 1(b). The pole figure indicates a bimodal distribution of basal poles, and the maximum intensity (5.20 a.u.) is found at locations tilted ±35° from the ND toward TD. It means that the *c*-axes of many grains in the sample lie about 35° to the normal direction of the sheet. It is a typical texture that can be commonly found in the cold rolled CP-Ti [16].

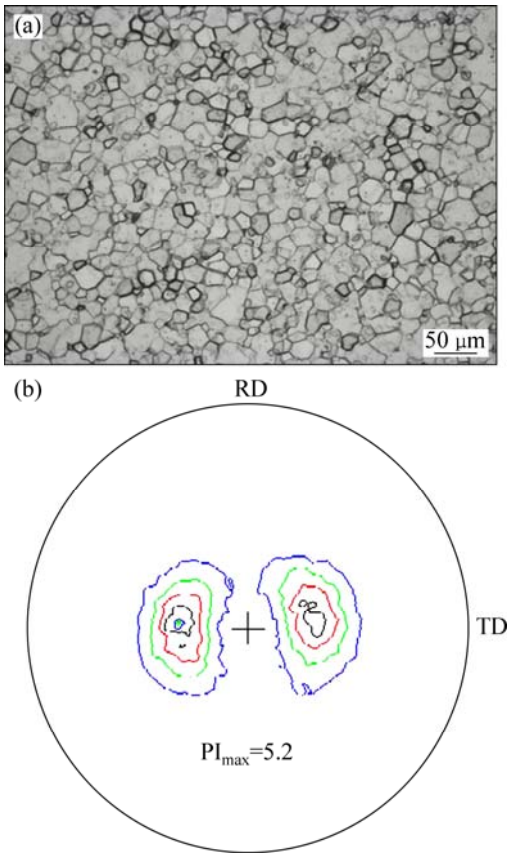

Fig. 1 Microstructure and texture of initial CP-Ti sheet: (a) Optical microstructure; (b) Measured (0002) pole figure obtained by XRD, (PI$_{max}$=maximum pole intensity); Contour levels (a.u.): 1.0, 2.0, 3.0, 4.0 and 5.0)

2.2 Forming process of drawn part

The deep drawing of the hemispheric surface part was performed at room temperature on a 500 t hydraulic machine. In order to obtain good deformation quality, the drawing velocity and lubrication conditions must be optimized. Figure 2 shows the hemispheric drawn part with a 6−8 cm flange, which was made at the drawn velocity of 4 mm/s. The height of the hemispheric surface part is 170 mm and the drawing ratio comes to 1.6. The thickness distribution of the drawn part measured along the rolling direction of initial sheet is shown in Fig. 3. It can be seen that the thickness reduction is quite small from the crown to the height of 60 mm (stretching region), but the reduction markedly increases in the drawing region, and the thickness at the flange almost has no change. In the stretching region, the thickness reduction is quite small since stretching is the predominant deformation mode. With the decreasing of the height, drawing becomes the predominant deformation mode and the thickness reduction increases. The reduction reaches the climax at the corner of wall.

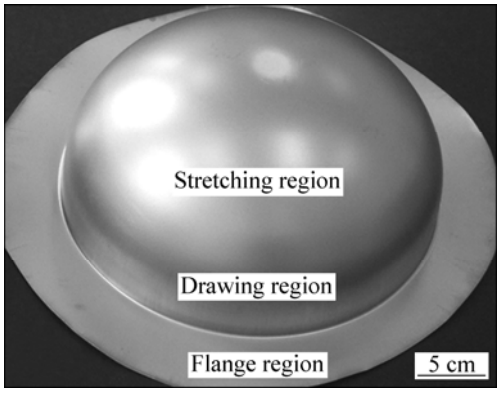

Fig. 2 Hemispheric surface part obtained after deep drawing

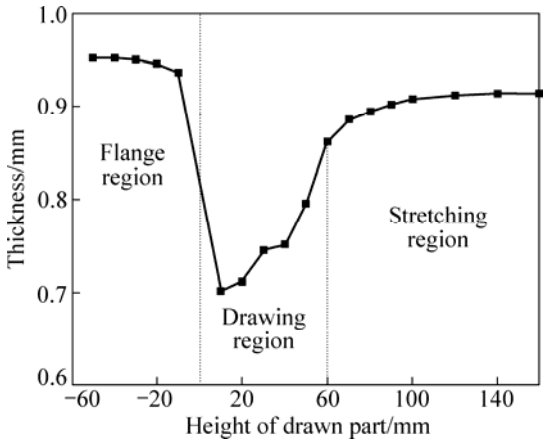

Fig. 3 Thickness reduction of drawn part from crown to flange

To be the representative of stretching region, drawing region and flange region, the samples were cut from the drawn part at the height of 160 mm, 20 mm, and at the flange of 10 mm away from the drawn part wall along the initial sheet's rolling direction.

2.3 Texture test and microstructure observation

In this study, the microstructure was investigated by OM and TEM. The OM samples were treated by mechanically polishing and electro-polishing. The electro-polishing was performed at room temperature using a DC power supply with 30 V, and the solution was constituted with 20 mL perchloric acid, 120 mL methanol and 60 mL butanol. The chemical etching solution was composed of 4 mL HNO_3, 2 mL HF and 94 mL H_2O. For TEM study, the rods with diameter of 3 mm cut from the sheets and deformed part were ion-thinned. And the TEM foils were studied on a Tecnai G2 F30 electron microscope operating at voltage of 300 kV.

The texture of the sheet and the deformed part was tested by XRD. A Siemens D5000 X-ray diffractometer equipped with Cu-monochromator was used. The samples were prepared in the size of 15 mm (RD)×10 mm (TD). Firstly, four pole figures (0002), (10 $\bar{1}$ 0), (10 $\bar{1}$ 1), (10 $\bar{1}$ 2) were obtained using the Schulz reflection method, then the orientation distribution function (ODF) was calculated using the series expansion method with L_{max}=16. The ODFs were present in the form of iso-intensity contour lines which represent the orientation densities in constant φ_2 sections. The pole figure calculated by ODF method was compared with the measured one to verify the reliability of the ODFs result.

3 Results and discussion

3.1 Microstructure of drawn part

In order to analyze the deformation mechanism of deep drawing process, the microstructures of three regions were observed, respectively. The sampling plan is shown in Fig. 4. The complex strain in the drawn part mainly consists of radial strain (ε_r) and tangential strain (ε_θ). According to the deformation mode shown in Fig. 5 and constant volume theory, the two strains can be calculated by:

$$\varepsilon_\theta = \frac{2\pi(R_{A0} - R_A)}{2\pi R_{A0}} \tag{1}$$

$$\varepsilon_r = -\frac{r+1}{r}\varepsilon_\theta \tag{2}$$

where r is the plastic strain ratio; R_{A0} and R_A are the distance between origin point (o) and A_0, A, respectively; A_0 and A are the points in the initial sheet and deformed part.

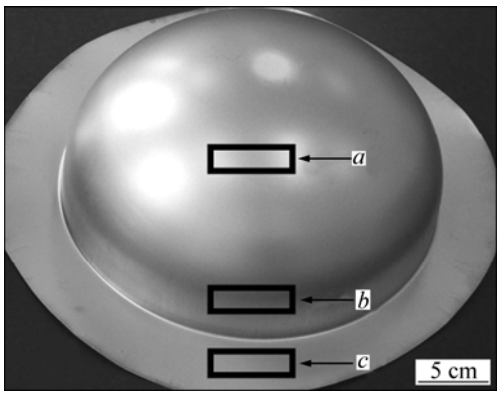

Fig. 4 Sketch of sampling plan

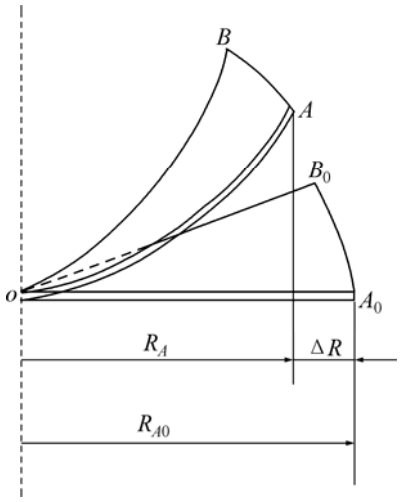

Fig. 5 Schematic diagram of deformation analysis

Figure 6 shows the microstructure in the stretching region cut from the height of 160 mm (region "*a*" in Fig. 4). Tangential compression and radial tension are the main deformation modes in this section. If we set r=1, the radial and tangential strains calculated by Eqs. (1) and (2) are 0.053 and −0.0265, respectively. It can be seen from Fig. 6(a) that the size and shape of the grains almost have no change, except few twins are produced in the grains (Fig. 6(b)). It means that the strain introduced in the stretching region is very small. Thereby, the dislocations present short rod like and the density is quite small (Figs. 6(c) and (d)).

However, as shown in Fig. 7(a), the grains in the drawing region (cut from region "*b*" in Fig. 4) are severely elongated along the radical direction. According to the thickness distribution curve shown in Fig. 3, the greatest thickness reduction and strain are produced at this section. The twins are introduced not only inside the grains, but also across the grain boundaries (Fig. 7(b)). And the density of twins is increasing substantially compared to the stretching region. Figures 7(c) and (d) show the distribution of dislocation cells and walls near the grain boundaries, respectively. It is observed that

drawing strain (0.21) is severe and the residual stress is quite large.

Figure 8 shows the microstructures from the flange part (region "*c*" in Fig. 4). Although the thickness reduction of flange region is the smallest, the grains are elongated along the radial direction and some twins are also generated inside the grains (Figs. 8(b) and (c)). As shown in Fig. 8(d), the dislocations in the flange region

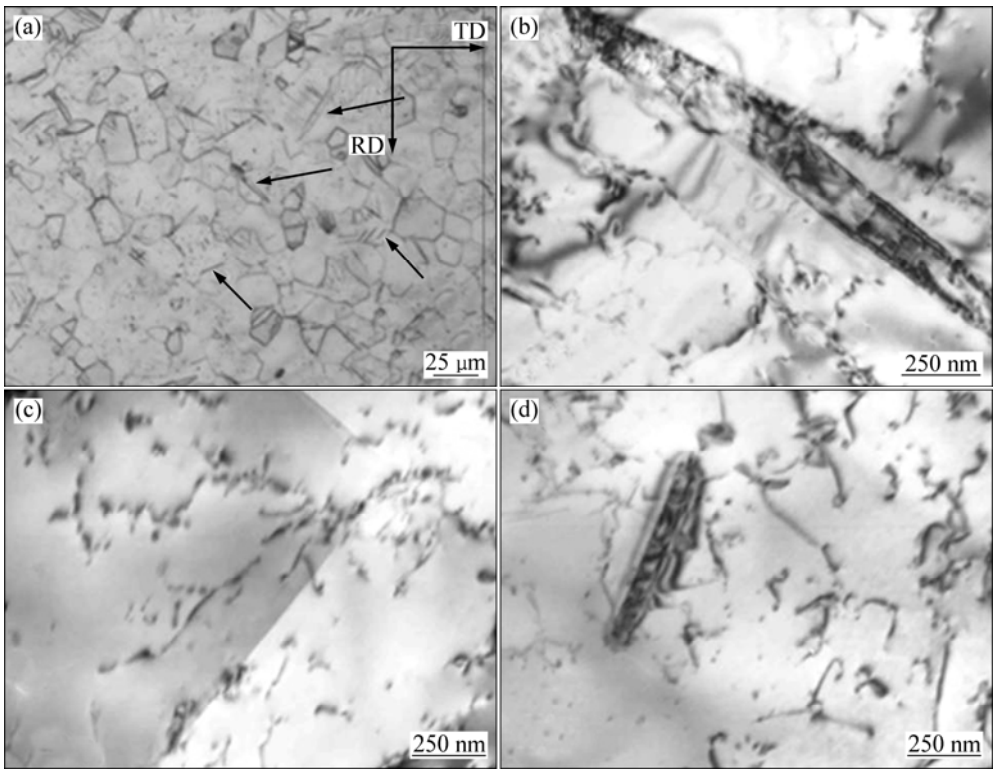

Fig. 6 Microstructures in stretching region of drawn part: (a) OM observation; (b) Deformation twinning produced inside grain; (c) Dislocations near grain boundary; (d) Dislocation around twinning

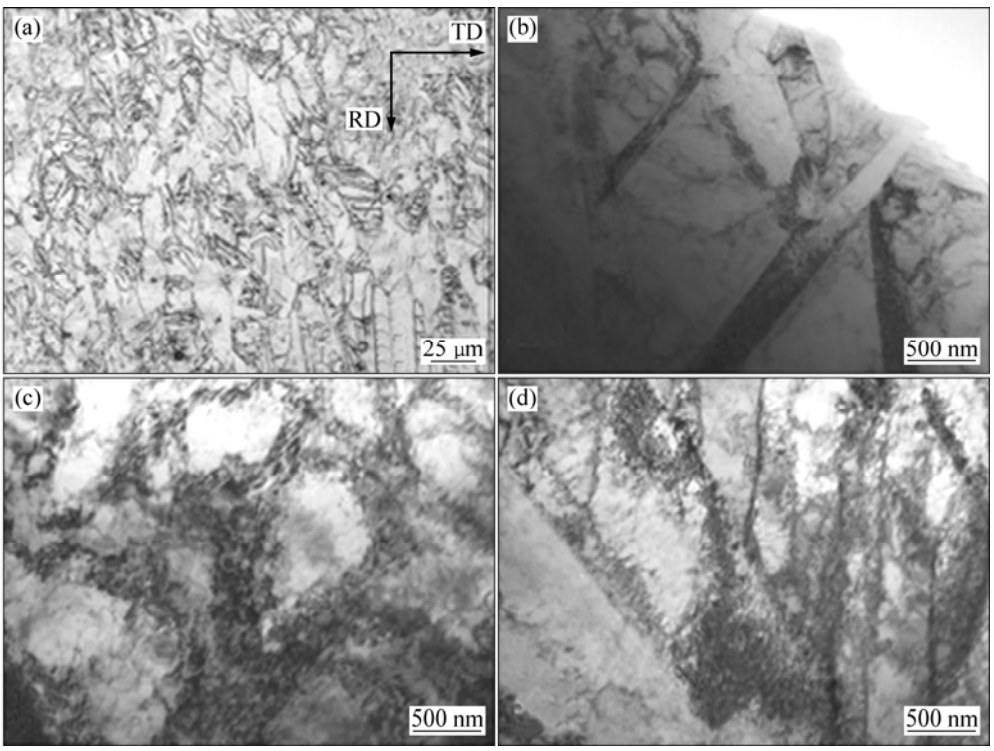

Fig. 7 Microstructures in drawing region of drawn part: (a) OM observation; (b) Distribution of deformation twinning; (c) Dislocation cells; (d) Dislocation walls around grain boundaries and sub-boundaries

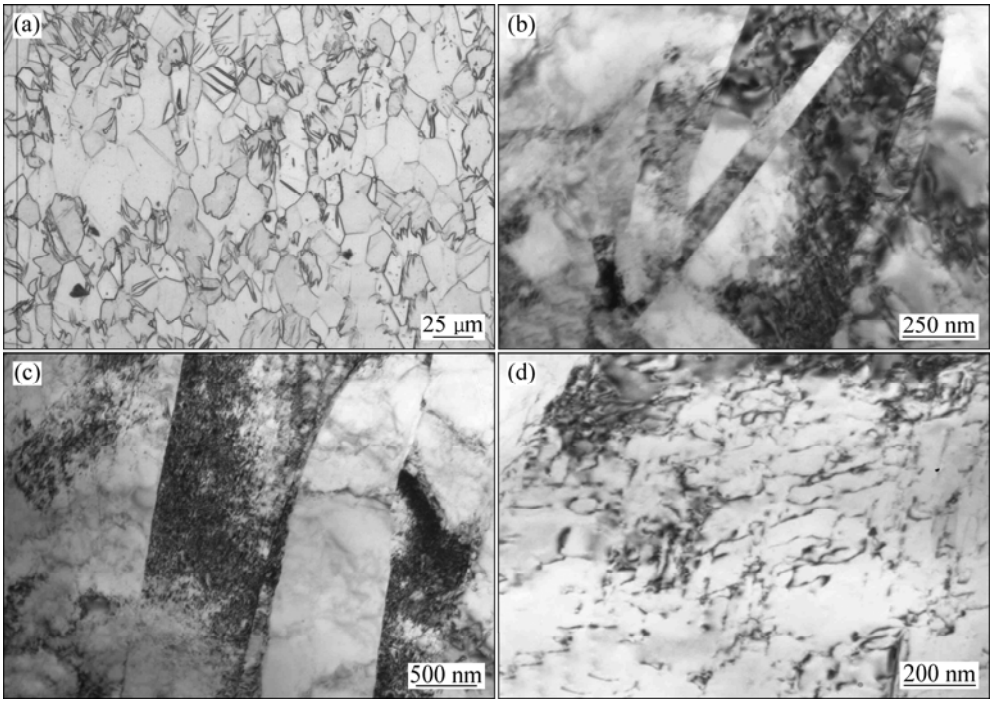

Fig. 8 Microstructures of flange region: (a) OM observation; (b), (c) Twinning in grain; (d) Distribution of dislocation

are orientated along the radial direction and the density is higher than that in the stretching region. This presents that the strain introduced in the flange region is greater than that in the stretching region. According to the loading mode, the strain in the flange region is produced by drawing along the radial direction and the pressure-pad-force normal to the drawing direction.

Deep drawing process of hemispheric part is a complex process including stretching and deep drawing, which is different from the normal drawing. The maximal plastic strain and thickness reduction are produced at the bottom of part and the wall region near the die corner. Great differences between deformation modes lead to unequal distribution of strain and result in different microstructure evolution process. The plastic strain is accommodated by dislocation slip and deformation twinning in the whole deep drawing process.

3.2 Texture development during deep drawing

The development of texture during drawing process was also interpreted in terms of the φ_2=0° and φ_2=30° sections of ODF maps (Fig. 9). The main texture component and the orientation density are shown in Table 2. In Table 2, the rolling texture is represented by A, B, D and E, while the component of recrystallization texture was denoted by C.

As shown in Fig. 9 and Table 2, the location of the maximum intensity progressed from (ϕ_1=15°, ϕ=24° and φ_2=0°) in the initial (undeformed) condition toward (ϕ_1=0°, ϕ=36° and φ_2=0°) in the stretching region, (ϕ_1=0°, ϕ=48° and φ_2=0°) in the drawing region and (ϕ_1=0°, ϕ=36° and φ_2=0°) in the flange region.

The texture of CP-Ti sheet usually consists of two parts, rolling texture (introduced in the cold rolling process) and recrystallization texture (introduced in the annealing process) [16,17]. In this study, the rolling texture of CP-Ti sheet contains two components, $(\bar{1}2\bar{1}7)[\bar{4}310]$ and $(\bar{1}2\bar{1}4)[10\bar{1}0]$, and the recrystallization texture is in $(01\bar{1}3)[3\bar{2}\bar{1}0]$ type. Compared to the drawn part, the rolling texture of the initial sheet has the largest maximum intensity of 12.221. After deep drawing, the texture component and the orientation density change in different locations of the drawn part. In the stretching region, the rolling texture changes to $(\bar{1}2\bar{1}5)[10\bar{1}0]$ without any intensity variation; however, the maximum intensity of the recrystallization texture decreases from 10.587 to 6.227. As a result of high drawing strain, the rolling texture changes to $(\bar{1}2\bar{1}3)[10\bar{1}0]$ with the maximum intensity reduced to 10.66 in the drawing region, and the recrystallization texture disappears. In the flange region, the maximum intensity values of the rolling texture and recrystallization texture reduces to 9.336 and 9.696, respectively.

According to the results of microstructure and texture investigation, the intensity reduction of texture is caused by twinning. Twinning weakens the initial texture component by randomizing the orientations of crystals [18]. Especially, this weakening effect is more obvious for recrystallization texture. Due to the significant forming of twinning, the recrystallization texture in the drawing region disappears. However, a larger drawing

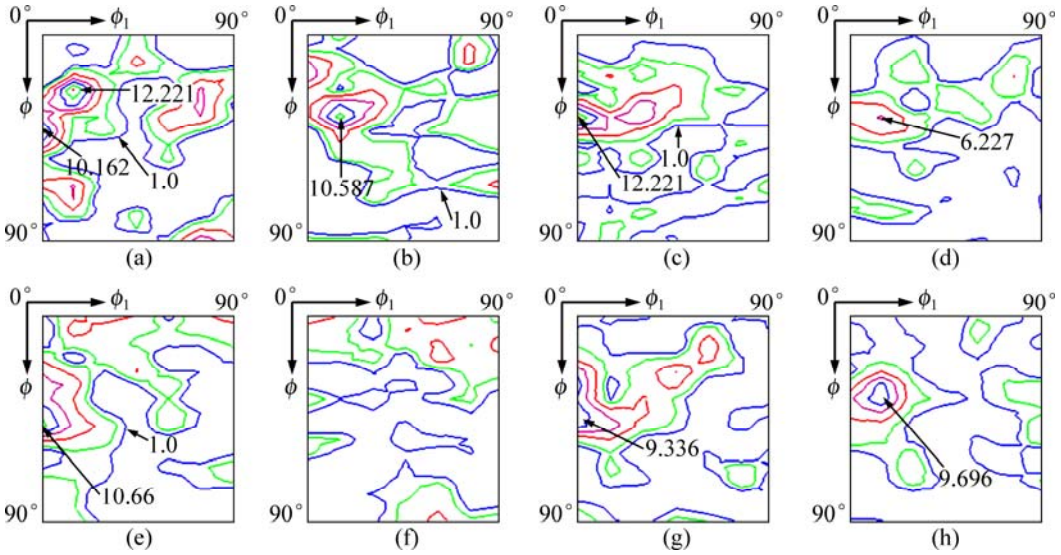

Fig. 9 ODF maps: (a) φ_2=0°, initial sheet; (b) φ_2=30°, initial sheet; (c) φ_2=0°, stretching region; (d) φ_2=30°, stretching region; (e) φ_2=0°, drawing region; (f) φ_2=30°, drawing region; (g) φ_2=0°, flange region; (h) φ_2=30°, flange region

Table 2 Texture component and orientation density of initial sheet and drawn part

Sample	Euler angle	Texture component	Orientation density
Initial sheet	A (15°,24°,0°)	$(\bar{1}2\bar{1}7)[\bar{4}310]$	12.221
	B (0°,40°,0°)	$(\bar{1}2\bar{1}4)[10\bar{1}0]$	10.162
	C (15°,36°,30°)	$(01\bar{1}3)[3\bar{2}\bar{1}0]$	10.587
Stretching region	D (0°,36°,0°)	$(\bar{1}2\bar{1}5)[10\bar{1}0]$	12.221
	C (15°,36°,30°)	$(01\bar{1}3)[3\bar{2}\bar{1}0]$	6.227
Drawing region	E (0°,48°,0°)	$(\bar{1}2\bar{1}3)[10\bar{1}0]$	10.66
Flange region	B (0°,40°,0°)	$(\bar{1}2\bar{1}4)[10\bar{1}0]$	9.336
	C (15°,36°,30°)	$(01\bar{1}3)[3\bar{2}\bar{1}0]$	9.696

strain may start and strengthen the texture component of (ϕ_1=0°, ϕ=48° and φ_2=0°), although the formation texture could be weakened by twinning.

The texture investigation of CP-Ti sheet reveals that the deformation twinning predominates the plastic strain in the stretching region and flange region, so the cold rolling texture is weakened. However, in the drawing region, the dislocation slip is activated in addition to twinning, and one of the deformation texture components is strengthened.

4 Conclusions

1) For the deep drawing process of CP-Ti sheet, the external strain is accommodated by dislocation slip and deformation twinning. In the stretching region, the plastic strain introduced by tangential and radial tension is quite small with a little deformation twinning and small quantity of dislocations. In the drawing region, the strain is so large that the grains are elongated along the radical direction with a lot of twinning and dislocation cells distributed in the microstructure. Moreover, in the flange region, the dislocations are orientated along the radial direction and the density is high than the stretching region, although the thickness reduction of flange region is smaller.

2) The texture of CP-Ti sheet and its drawn part consists of rolling texture component and recrystallization texture. In the drawing process, the location of the maximum intensity progresses from (ϕ_1=15°, ϕ=24° and φ_2=0°) in the initial condition toward (ϕ_1=0°, ϕ=36° and φ_2=0°) in the stretching region, (ϕ_1=0°, ϕ=48° and φ_2=0°) in the drawing region and (ϕ_1=0°, ϕ=36° and φ_2=0°) in the flange region.

3) Twinning weakens the initial texture by randomizing the orientations of crystals, especially for the recrystallization texture. The recrystallization texture in the drawing region disappears due to the significant forming of twinning. Furthermore, deep drawing will result in the predominance of the dislocation slip and strengthen the texture. In this study, the characteristic deformation texture of (ϕ_1=0°, ϕ=48° and φ_2=0°) is a consequence of deformation by slip.

References

[1] GERD L, JAMES C W. Titanium [M]. 2nd ed. Berlin, Heidelberg: Springer-Verlag, 2007: 180−201.

[2] MORI K, MURAO T, HARADA Y. Multi-stage cold deep drawing of long pure titanium cups using colored sheets for prevention of seizure [J]. CIRP Annals Manufacturing Technology, 2003, 52(1):

237−240.
[3] TAM W H, BALLINGER I A, KOHORST P. Design and manufacture of a composite overwrapped elastomeric diaphragm tank [R]. Commerce, CA: PSI, 2004.
[4] BENTON J F, DEBRECENI M. Design modification of a diaphragm propellant tank for a pressurant tank application [R]. Commerce, CA: PSI, 2004.
[5] CHEN F K, CHIU K H. Stamping formability of pure titanium sheets [J]. Journal of Materials Processing Technology, 2005, 170(1−2): 181−186.
[6] XU C, ZHU W F. Transformation mechanism and mechanical properties of commercially pure titanium [J]. Transactions of Nonferrous Metals Society of China, 2010, 20(11): 2162−2167.
[7] LIU J M, CHOU S S. Study on the microstructure and formability of commercially pure titanium in two temperature deep drawing [J]. Journal of Materials Processing Technology, 1999, 95(1−3): 65−70.
[8] ZENG Z P, ZHANG Y S, JONSSON S. Deformation behaviour of commercially pure titanium during simple hot compression [J]. Materials and Design, 2009, 30(8): 3105−3111.
[9] KIM W J, YOO S J, JEONG H T, KIM D M, CHOE B H, LEE J B. Effect of the speed ratio on grain refinement and texture development in pure Ti during differential speed rolling [J]. Scripta Materialia, 2011, 64(1): 49−52.
[10] ZHU X J, TAN M J, ZHOU W. Enhanced superplasticity in commercially pure titanium alloy [J]. Scripta Materialia, 2005, 52(7): 651−655.
[11] SUWAS S, BEAUSIR B, TOTH L S, FUNDENBERGER J J, GOTTSTEIN G. Texture evolution in commercially pure titanium after warm equal channel angular extrusion [J]. Acta Materialia, 2011, 59(3): 1121−1133.
[12] SATOH J, GOTOH M, MAEDA Y. Stretch-drawing of titanium sheets [J]. Journal of Materials Processing Technology, 2003, 139(1−3): 201−207.
[13] ZHANG X H, TANG B, LI J S, KOU H C, ZHOU Z B, CHEN W, CHEN B, ZHOU L. Deformation numerical simulation of titanium diaphragm for spacecraft tank [J]. Journal of Astronautics, 2010, 31(9): 2184−2188. (in Chinese)
[14] LIU Y L, CHU J Y, FU S. Experimental study of the deformation laws of hemispherical parts in the compound-forming process [J]. Journal of Materials Processing Technology, 1998, 74(1−3): 190−194.
[15] GAO E Z, LI H W, KOU H C, CHANG H, LI J S, ZHOU L. Influences of material parameters on deep drawing of thin-walled hemispheric surface part [J]. Transactions of Nonferrous Metals Society of China, 2009, 19(2): 433−437.
[16] ZHU Z S, CU J L, CHEN N P. On the texture controlling methods and mechanical property anisotropy in commercially pure titanium sheet [J]. Materials for Mechanical Engineering, 1994, 18(6): 8−11. (in Chinese)
[17] ZHU Z S, CU J L, CHEN N P. Research on the relationship between texture and mechanical property anisotropy in commercially pure titanium sheets [J]. Materials for Mechanical Engineering, 1994, 18(2): 23−26. (in Chinese)
[18] CHUN Y B, YU S H, SEMIATINB S L, HWANG S K. Effect of deformation twinning on microstructure and texture evolution during cold rolling of CP-titanium [J]. Materials Science and Engineering A, 2005, 398 (1−2): 209−219.

纯钛板材冷拉成形过程中的微观组织与织构演变

张绪虎，唐 斌，张下陆，寇宏超，李金山，周 廉

西北工业大学 凝固技术国家重点实验室，西安 710072

摘 要：研究纯钛板材冷拉成形过程中微观组织及织构演化规律。半球形壳体件在深拉延过程中由于各部位变形模式及应变形式的不同会形成胀形区、拉深区及法兰区等 3 个区域。结果表明，在拉深件的 3 个区域中塑性应变均由位错滑移与变形孪晶共同作用。纯钛板材及其拉深件中的织构包含轧制织构与再结晶织构。由于变形孪晶与位错滑移对织构的影响规律不同，初始板材织构的强度及类型在深拉过程中不断变化。变形孪晶对初始织构具有弱化作用，特别是对于再结晶织构，这种弱化效应更为明显。由于拉深区产生的孪晶较多，再结晶织构消失。此外，大拉伸变形时位错滑移为主导机制，织构强化效应明显。

关键词：纯钛；深拉延；微观组织；织构

(Edited by YUAN Sai-qian)